Chapter 3
Tropospheric Modeling from GPS

Abstract The dynamics of the neutral atmosphere is of great interest to a meteorologist who predicts weather and climatologist who performs climate modeling. Modeling the effect of GPS signals for the above applications require information about the properties of the atmosphere. This chapter provides a modeling of tropospheric delay from the effect of the propagation GPS signals in the atmosphere. The modeling will include the overview of the empirical models of zenith tropospheric delay together with the mapping function.

Keywords Atmosphere · GPS signals · Refractive index · Tropospheric delay modeling · Mapping function

3.1 The Neutral Atmosphere and Its Composition

Monitoring of the dynamics of the atmosphere shows that they are composed of several chemically distinct gasses, the relative amounts of which within the lower atmosphere may be determined. The composition and structure of this unique resource are important keys to understanding circulation in the atmosphere, short-term local weather patterns and long-term global climate changes.

Characterizing the atmosphere, by the way, radio wave is propagated that leads to a subdivision of neutral atmosphere and ionosphere. The neutral atmosphere layer consists of three temperature-delineated regions: the troposphere, the stratosphere and part of the mesosphere. It is often simply referred to as the *troposphere* because in radio wave propagation, the troposphere effects dominate. Hence, to the GPS researcher, the "troposphere" is generally referred to the neutral atmosphere at altitudes 0–40 km (Gregorius and Blewitt 1999). On the other hand, when speaking of the troposphere, it will be clear from the context, whether it referred to the neutral atmosphere or the specific layer.

The layers of the troposphere are defined by their characteristics such as temperature, pressure, and chemical composition. Pressure and density decrease as a

W. Suparta and K.M. Alhasa, *Modeling of Tropospheric Delays Using ANFIS*,
SpringerBriefs in Meteorology, DOI 10.1007/978-3-319-28437-8_3

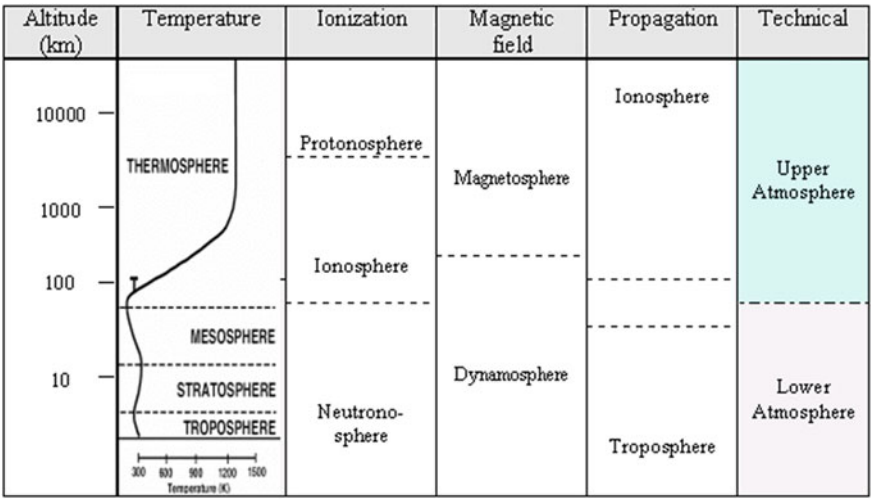

Fig. 3.1 Possible subdivision schemes of the Earth's atmosphere adapted from Seeber (1993)

function of altitude following the exponential barometric law. In general, the temperature in the troposphere decreases linearly with height at a rate of 6.5 °C km^{-1} (on average). The actual value of this temperature gradient is a function of height, season and geographical location. At the top of the *troposphere*, at a boundary layer between 12 and 18 km (mean sea level, MSL), the temperature remains approximately constant at a level of −60 to −80 °C. However, this boundary still has weather such as clouds formation and precipitation, wind blows, and the atmosphere interacts with the surface of the Earth below. This part of the neutral atmosphere is called the *tropopause*. The upper part above the tropopause is referred to as the *stratosphere*, up to an altitude of 40 km temperature increases again in the stratosphere up about 50 km altitude (as the *mesosphere*). The stratosphere is mainly responsible for absorbing the ultraviolet radiation. Between 50 and 80 km above MSL, the temperature drops again in the mesosphere. At the outer reaches of the Earth, atmosphere is the *thermosphere* with an initial slow temperature increase. Figure 3.1 shows the detailed subdivisions of the atmosphere with characteristic features such as temperature, ionization, and propagation (Seeber 1993).

3.2 Tropospheric Delay Modeling

Yuan et al. (1993) described that the troposphere affects the propagation of GPS radio signals in two ways. First, waves travel slower in the atmosphere ('bending effect') than they are in free-space. Second, they travel in a curved path rather than a straight-line ('geometrical delay or excess path delay'). Both effects arise

significantly due to the refractivity variations in the atmosphere along the ray path and the modeling will take into account of these effects.

3.2.1 Refraction of GPS Signals in the Troposphere

Refraction effects are generally caused by an inhomogeneous propagation medium. The refractive index is often thought of as an "optical density" and for the ordinary ray it is constant and independent of direction. When the radio signals traverse the Earth's atmosphere, they are affected significantly by variations in the refractive index of the troposphere. Refraction bends the ray path and thereby lengthens it, further increasing the delay. The refractive index of a material is the factor by which the phase velocity of electromagnetic radiation is slowed in that material, relative to its velocity in a free-space. The tropospheric propagation delay can be determined from models and approximations of the atmospheric profiles.

The refractive index of the troposphere is constituent of gasses slightly greater than unity. The resulting decrease in velocity increases the time taken for signal to reach a receiver's antenna, thereby increasing the equivalent path length. The combination of these two effects is called the troposphere refraction component of propagation delay. Both L1 and L2 frequencies of GPS are affected by atmospheric refraction. This refractive delay obtained from biases between the satellite receiver range measurements.

3.2.1.1 Refractive Index

Like all electromagnetic waves, the ranging signals broadcasted by the GPS satellites can be described by Maxwell's equations. The propagation media in the equations are characterized by the magnetic permeability (μ) and the electric permittivity (ε). The velocity of an electromagnetic wave is characterized by the refractive index, n. These represent the ratio of the free-space speed (c) of electromagnetic wave to its media speed (v) and are related by Maxwell's equation (Brunner 1993). Therefore, the refractive index of a medium is given as

$$n = \frac{c}{v}\sqrt{\varepsilon\,\mu} \tag{3.1}$$

Solution of Maxwell's equation can be difficult to obtain if μ and ε are functions of position. Basically, Snell's Law equation is commonly used to determine a refractive index for a simple case with two or three different mediums. However, one method based on the first principle of Newton's second law (see Griffith 1999) can be used to show where the neutral part of atmosphere acts as a nondispersive medium for the radio frequency.

3.2.1.2 Refractivity

The refractivity of the atmosphere determines the amount of "bending" of the radio waves. The refractive index of moist air is different from unity because its constituents suffer polarization induced by the electromagnetic field of the radio signals. As the electromagnetic waves in the atmosphere propagate just slightly slower than in a free-space, the refractive index is close to unity in the terrestrial atmosphere. It is convenient to define the refractivity (Brunner 1993):

$$N = 10^6(n-1) \tag{3.2}$$

where n is the refractive index of radio wave in an air at ambient condition and N is the total refractivity of radio wave.

In the equation of state, total refractivity is a function of temperature, partial pressure of dry air, and partial pressure of water vapor that can be derived using the following expression (Smith and Weintraub 1953):

$$N = N_{\mathrm{d}} + N_{\mathrm{w}} = \underbrace{k_1 \frac{P_{\mathrm{d}}}{T_{\mathrm{K}}}}_{\text{dry}} + \underbrace{\underbrace{k_2 \frac{P_{\mathrm{w}}}{T_{\mathrm{K}}}}_{\text{dipole moment}} + \underbrace{k_3 \frac{P_{\mathrm{w}}}{T_{\mathrm{K}}^2}}_{\text{dipole oritentation}}}_{\text{wet}} \tag{3.3}$$

where k_i (i = 1…3) is the refraction constants are empirically determined and the most significant recent evaluations of the refractivity constants are summarized in Table 3.1, P_{d} is the partial pressure of dry air (mbar), T_{K} is the surface air temperature (Kelvin) and P_{w} is the partial pressure of water vapor (mbar).

Thayer (1994) took into account the nonideal gaseous behavior of the atmosphere and improved the refractivity formula as shown in Eq. 3.3. This reduced the computation uncertainty of 0.6 % before down to 0.02 %. Therefore, the refractivity N can be written as

$$N = k_1 \left(\frac{P_{\mathrm{d}}}{T_{\mathrm{K}}}\right) Z_{\mathrm{d}}^{-1} + \left(k_2 \frac{P_{\mathrm{w}}}{T_{\mathrm{K}}} + k_3 \frac{P_{\mathrm{w}}}{T_{\mathrm{K}}^2}\right) Z_{\mathrm{w}}^{-1} \tag{3.4}$$

Table 3.1 Determinations of the refractivity constants (Bevis et al. 1994; Suparta 2008)

Reference	k_1 (K mbar^{-1})	k_2 (K mbar^{-1})	k_3 (K^2 mbar^{-1}) × 10^5
Smith and Weintraub (1953)	77.61 ± 0.01	72 ± 9	3.75 ± 0.03
Boudouris (1963)	77.59 ± 0.08	72 ± 11	3.75 ± 0.03
Thayer (1974)	77.61 ± 0.01	47.79 ± 0.08	3.776 ± 0.04
Hill et al. (1982)	–	98 ± 1	3.583 ± 0.03
Hill (1988)	–	102 ± 1	3.578 ± 0.03
Clynch (1990)	77.604 ± 0.02	75 ± 0.1	3.75 ± 0.01
Bevis et al. (1992)	77.60 ± 0.05	70.4 ± 2.2	3.739 ± 0.012
Bevis et al. (1994)	77.60 ± 0.09	69.4 ± 2.2	3.701 ± 1200

In the above equation, P_w is obtained from relative humidity (H) as recommended by World Meteorological Organization Technical Note No. 8 (WMO 2000) and given by

$$P_w = \frac{H}{100}\exp\left(-37.2465 + 0.213166\,T_K - 2.56908\,\times\,10^{-4}\,T_K^2\right) \tag{3.5}$$

Both the dimensionless Z_d^{-1} and Z_w^{-1} are the inverse compressibility factors for dry air and water vapor constituents, respectively, to account for nonideal gas behavior. They have been experimentally determined by Owens (1967) and given as follows

$$Z_d^{-1} = 1 + (P - P_w)\left[57.97 \times 10^{-8}\left(1 + \frac{0.52}{T_K}\right) - 9.4611 \times 10^{-4}\frac{T}{T_K^2}\right] \tag{3.6}$$

$$Z_w^{-1} = 1 + 1650\frac{P_w}{T_K^3}\left(1 - 0.01317\,T + 1.75 \times 10^{-4}\,T^2 + 1.44 \times 10^{-6}\,T^3\right) \tag{3.7}$$

The first term of the Thayer Eq. 3.4 can be reformulated as a function of total moist air density (ρ_{tot}), allowing its direct integration by applying the hydrostatic equation (Davis et al. 1985). Consequently, the refractivity constant k_2 is also substituted with a new constant k_2' (Bevis et al. 1994) and the final expression for the total refractivity can be given as a sum of a hydrostatic (as opposed to dry) and wet components. The expression for total refractivity from Eq. 3.4 can be rewritten by separating the dry and wet terms as follows:

$$N = \underbrace{k_1\left(\frac{P_d}{T_K}\right)Z_d^{-1}}_{\text{dry}} + \underbrace{\left(k_2\frac{P_w}{T_K} + k_3\frac{P_w}{T_K^2}\right)Z_w^{-1}}_{\text{wet}} \tag{3.8}$$

By introducing ρ_{tot} (Wallace and Hobbs 1997) and measured quantity of pressure, P is, respectively, given as

$$\rho_{tot} = \rho_d + \rho_w \quad \text{and} \quad P = P_d + P_w \tag{3.9}$$

The first ideal gas equation, applied to dry air (ρ_d) and water vapor (ρ_w) were introduced by Spilker (1996), respectively.

$$P_d = \rho_d R_d T_K Z_d \quad \text{and} \quad P_w = \rho_w R_w T_K Z_w \tag{3.10}$$

A relation between molar mass of dry air and water vapor, and universal gas constant in the equation of state for ideal gasses in Eq. 3.10 can be approximated by

$$R_d = \frac{R}{M_d}, \quad R_w = \frac{R}{M_w}, \quad \text{and} \quad \frac{R_d}{R_w} = \frac{M_w}{M_d} \tag{3.11}$$

Let us now consider the dry part of the refractivity formula in Eq. 3.8

$$k_1\left(\frac{P_d}{T_K}\right)Z_d^{-1} = k_1\frac{P_d}{T_K}\frac{\rho_d R_d T_K}{P_d} = k_1(\rho_{tot} - \rho_w)R_d = k_1\rho_{tot}R_d - k_1\rho_w R_d \quad (3.12)$$

Considering the ideal gas equation for water vapor in the Eqs. 3.10 and 3.11, Eq. 3.12 can be written as

$$k_1\left(\frac{P_d}{T_K}\right)Z_d^{-1} = k_1\rho_{tot}R_d - k_1\frac{P_w}{T_K}\frac{M_w}{M_d}Z_w^{-1} \quad (3.13)$$

Substitution of this expression into the total refractivity formula in Eq. 3.8 yields

$$N = k_1 R_d \rho_{tot} + \left(k_2\frac{P_w}{T_K} - k_1\frac{P_w}{T_K}\frac{M_w}{M_d} + k_3\frac{P_w}{T_K^2}\right)Z_w^{-1} \quad (3.14)$$

where the dry inverse compressibility factor is eliminated. The total refractivity is then given as

$$N = k_1 R_d \rho_{tot} + \left(k_2'\frac{P_w}{T_K} + k_3\frac{P_w}{T_K^2}\right)Z_w^{-1} \quad (3.15)$$

with

$$k_2' = k_2 - k_1\frac{M_w}{M_d} = (22.1 \pm 2.2) \quad (3.16)$$

where R is the universal gas constant (8314.34 J kmol^{-1} K^{-1}), R_d is the specific gas constant for dry air (287.054 J kg^{-1} K^{-1}), R_w is the specific gas constant for water vapor (461.5184 J mol^{-1} K^{-1}), ρ_{tot} is the total mass density (moist air density) of the troposphere (kg m^{-3}), ρ_d is the density of dry air (kg m^{-3}), ρ_w is the density of water vapor (kg m^{-3}), M_w is the molar mass of water vapor (28.9644 kg kmol^{-1}), and M_d is the molar mass of dry air (18.0152 kg kmol^{-1}). Expanding on development of refractivity as a function of wet and hydrostatic components, it is possible to examine their individual contribution to the tropospheric path delay.

3.2.2 Tropospheric Path Delay

There are two main parameters which play an important role during the propagation between transmitter (GPS) and receiver: pseudorange and carrier phases. All these propagation effects and time offsets have to be determined to account accurate estimation of position from range data. Thus, to understand comprehensively about

tropospheric path delay modeling, the basic properties of radio waves propagation in the troposphere will first be described.

The basic physical law for the propagation is Fermat's principle: Light (or any electromagnetic wave) will follow the path between two points (P_1 and P_2 are ends of S) involving the least travel time. We define the electromagnetic (or optical) distance between source and receiver as

$$L = \int c\,\mathrm{d}t = \int \frac{c}{v}\mathrm{d}S = \int_S n(s)\mathrm{d}S \tag{3.17}$$

where L is the delay of radio wave (so-called optical path length or electromagnetic distance, total tropospheric delay), $n(s)$ is the index of refraction which varies as a function position along the curved ray path L, S is the electromagnetic path, $\mathrm{d}S$ is infinitesimal parts of the path length, and c and v are speed of the radio signals in free-space and in medium, respectively. If we denote the geometrical distance or the straight-line (rectilinear) path in a free-space by

$$G = \int_G \mathrm{d}G \tag{3.18}$$

where G is the geometrical distance and $\mathrm{d}G$ is an infinitesimal part of the path length in free-space.

Figure 3.2 shows the GPS signals traveling through the troposphere. The total delay, then, is the sum of these two components and can be written as

$$\Delta L = \int_S n(s)\,\mathrm{d}S - G \tag{3.19}$$

or,

$$\Delta L = \int_S (n(s) - 1)\mathrm{d}S - \int_G \mathrm{d}G \tag{3.20}$$

$$\Delta L = \underbrace{\int_S [n(s) - 1]\mathrm{d}S}_{\text{The slowing effect}} + \underbrace{[S - G]}_{\text{The bending effect}} \tag{3.21}$$

where ΔL is the total tropospheric delay stated in terms of equivalent increase in path length, S is the true path along L which the radio wave propagates and G is the

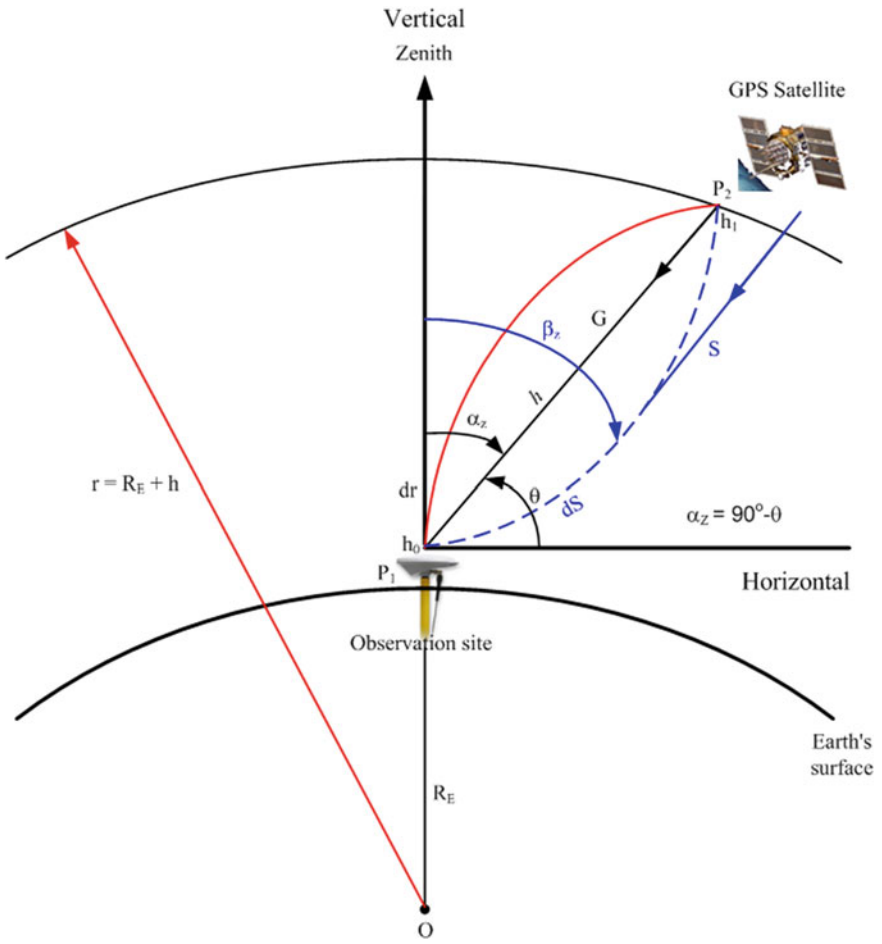

Fig. 3.2 GPS signals traveling through troposphere and the tropospheric path delay geometry (Suparta 2008)

shortest geometric path along which the signal would transverse, and assuming as $n = 1$. In the first term of Eq. 3.21, the integral is performed along the line increment dS of straight ray path (excess path delay) from a receiver to a GPS satellite.

The second term indicates the geometric delay due to ray path bending. The bending term $[S - G]$ is much smaller, about 1 cm or less, for path with elevation angle greater than 10°. Bending is about 1 mrad for a 15° elevation angle and its associated excess path length is about 1 cm, which is usually neglected since it represents $\sim$0.1 % of the total path delay (see Bock and Doerflinger 2001). For rays oriented along the zenith and in the absence of horizontal gradients in index

refractivity n, the ray path is straight-line and the bending term vanishes. Excess path length due to signal retarding in the troposphere in Eq. 3.21, or slant path delay (Davis 1985), is expressed as

$$\Delta L^z = \int_S [n(s) - 1] \mathrm{d}S \tag{3.22}$$

where ΔL^z is the total tropospheric delay in the zenith direction, which is referred as the ZTD.

However, in the troposphere several simplifying assumptions can be made to simplify Eq. 3.22. First, the atmosphere is assumed to be spherically symmetric, that is, the Earth is a sphere and the properties of the atmosphere vary only with geometric radius. In this way, the atmosphere can be considered layered with a refractive index characterizing each layer. Second, the atmosphere is usually assumed to be azimuthally symmetric, that is, with no variation of the refractive index in azimuth of each layer. In this way, the electromagnetic ray is confined to a plane defined by the start and end points of the ray and the geocentric. These assumptions allow us to represent the refractive index profile as a function of geocentric radial distance only, $n(h)$. On application of the refractivity in Eq. 3.2, Eq. 3.21 for S can then be written as

$$G + \Delta L^z = \int_{h_0}^{h_1} n(h) \sec \beta_z(h) \mathrm{d}h \tag{3.23}$$

where the refractive index is integrated along the path between points h_0 and h_1, which are the geocentric distance of the user's antenna and the geocentric distance of the 'top' of troposphere, respectively. Angle α_z is the true (unrefracted) satellite zenith angle and hence constant along the unrefracted path. Angle β_z is the actual (refracted) zenith angle of the ray path at distance h (see Fig. 3.2). The path delay is caused by variation of n from unity, hence

$$G + \Delta L^z = \int_{h_0}^{h_1} [n(h) - 1] \sec \beta_z(h) \mathrm{d}h + \int_{h_0}^{h_1} \sec \beta_z(h) \mathrm{d}h \tag{3.24}$$

This gives in the first term the excess delay equivalent path length and in the second term the geometric length along the curved path. To obtain the total tropospheric delay (ΔL^z), we can subtract the geometric distance in free-space to get the following integral equation (Langley 1996):

$$\Delta L^{z} = \underbrace{\int_{h_0}^{h_1} [n(h) - 1] \sec \beta_z(h) \mathrm{d}h}_{\text{symmetric}} + \left[\underbrace{\int_{h_0}^{h_1} \sec \beta_z(h) \mathrm{d}h - \int_{h_0}^{h_1} \sec \alpha_z \mathrm{d}h}_{\delta - \text{asymmtric}} \right] \tag{3.25}$$

To summarize, the first integral accounts for the difference between the electromagnetic distance and geometric distance along the ray path and the bracketed integrals account for curvature of the ray path, i.e., the difference between the refracted and rectilinear geometric distances. The total tropospheric delay by inserting Eq. 3.2, can be simplified as

$$\Delta L^{z} = 10^{-6} \int_{\text{actual}} N(h) \mathrm{d}h + \delta \tag{3.26}$$

For easy modeling of the tropospheric delay, the total refractivity at distance h, $N(h)$ in the troposphere can be explicitly written as the contribution of a wet (N_w) and a hydrostatic (N_h) component. Therefore, Eq. 3.26 can be written as

$$\Delta L^{z} = \left(\int N_h \mathrm{d}h + \int N_w \mathrm{d}h \right) 10^{-6} + \delta \tag{3.27}$$

and symbolically, as

$$\Delta L^{z} = (L_h + L_w) + \delta \tag{3.28}$$

where L_h represents the hydrostatic delay and L_w is the wet delay.

Propagation delays at arbitrary elevation angles are determined from the zenith delay and arecalled the "mapping functions." As the zenith delay can be expressed as the sum of the hydrostatic and wet components, mapping functions can be developed in order to map separately the hydrostatic and wet components. Tropospheric delays increase with decreasing satellite elevation angle. This is accounted for by multiplying the zenith delay by a correction factor, m. In general, total tropospheric delay from Eq. 3.28, following Davis et al. (1985), can be rewritten as

$$\Delta L^{z} = (m_h \mathrm{ZHD} + m_w \mathrm{ZWD}) + \delta \tag{3.29}$$

where ΔL^{z} is the total delay along the zenith path called zenith path delay (ZPD), sometimes called the zenith total delay (ZTD) or zenith tropospheric delay (m). ZHD and ZWD are the hydrostatic zenith delay and the wet zenith delay, which both in meter, and θ is the satellite elevation angle (degrees). The last symbol in Eq. 3.29, δ is the tropospheric correction (recently, known as a gradient

tropospheric delay, $\delta = m(\theta)\cot\theta\,[G_N\cos\alpha_z + G_E\sin\alpha_z]$ symmetric effects into account (δ = 0, the asymmetric components are neglected by setting the cutoff elevation angle ≥ 10°), and m is the obliquity factor from sec α_z ($\alpha_z = 90° - \theta$, is the azimuth angle), separated into m_h and m_w, the hydrostatic and wet mapping functions, respectively. G_N and G_E are the components of the gradient vector in the north and east directions, respectively.

3.3 Empirical Models of Tropospheric Delay

In the past several decades, a number of tropospheric propagation models have been reported in the scientific literature. Much research has gone into the creation and testing of tropospheric refraction models to compute the refractivity along the path of signal travel. The various tropospheric models differ primarily with respect to the assumption made regarding the vertical refractivity profiles and the mapping functions to map the delays to the arbitrary elevation angles. To model the tropospheric delay, many models use information about the surface pressure, temperature, and relative humidity to derive zenith or slant delay estimates. However, most models require certain conditions in, or make assumptions about, the atmosphere above the station. Among the commonly used models for the tropospheric delay are Saastamoinen (1972), Hopfield (1969), Modified Hopfield (Goad and Goodman 1974), Davis (1985), Herring (1992), Lanyi (1984), and Niell (1996, 2000). In this section, only the first three models are discussed. These models are most widely used due to their high accuracy, practicality, and suitable with the GPS measurements.

3.3.1 The Saastamoinen Model

The Saastamoinen model (SAAS) was developed for high elevation angles. This model has become popular among GPS users due to its accuracy. This model assumes that the atmosphere is in hydrostatic equilibrium, which follows from the ideal gas law. Under hydrostatic equilibrium, the local pressure, which is assumed isotropic, provides the balancing force against the atmospheric weight per unit area. Models for the ZTD, ZHD, and ZWD as derived by Saastamoinen (1972) will be described in this subsection.

Considering only the delay in the zenith direction, Eq. 3.25 reduces to

$$\Delta L^z = \mathrm{ZTD} = \int_{h_0}^{h_1} [n(h) - 1]\mathrm{d}h = 10^{-6}\int_{h_0}^{h_1} N(h)\mathrm{d}h \tag{3.30}$$

or, explicitly using Eq. 3.16,

$$\mathrm{ZTD} = \underbrace{10^{-6}\int_{h_0}^{h_1} k_1 R_\mathrm{d}\rho_\mathrm{tot}\mathrm{d}h}_{\text{hydrostatic}} + \underbrace{10^{-6}\int_{h_0}^{h_1}\left(\frac{k_2'}{T_\mathrm{K}}+\frac{k_3}{T_\mathrm{K}^2}\right)P_\mathrm{w}Z_\mathrm{w}^{-1}\mathrm{d}h}_{\text{wet}} \tag{3.31}$$

The first term in Eq. 3.31 represents the ZHD. By assuming a radio signal arrives from a zenith direction, the ZHD can be written as

$$\mathrm{ZHD} = 10^{-6}k_1 R_\mathrm{d}\int_{h_0}^{\infty}\rho_\mathrm{tot}(h)\mathrm{d}h \tag{3.32}$$

Under the condition of hydrostatic equilibrium, the hydrostatic equations is

$$\mathrm{d}P = -g(h)\rho_\mathrm{tot}(h)\mathrm{d}h \tag{3.33}$$

where $\mathrm{d}P$ is the differential change in surface pressure (mbar), $g(h)$ is the acceleration due to gravity as a function of height (ms^{-2}), $\rho_\mathrm{tot}(h)$ is the density of moist air as a function of height, and $\mathrm{d}h$ is the differential change in height (m).

Integrating Eq. 3.33 yields

$$\int_P^0 \mathrm{d}P = -\int_{h_0}^{\infty}\rho_\mathrm{tot}(h)g(h)\mathrm{d}h = -P \tag{3.34}$$

Introducing the weighted mean gravity acceleration, g_m, the ZHD can be written as

$$\mathrm{ZHD} = 10^{-6}k_1 R_\mathrm{d}\frac{P}{g_\mathrm{m}} \tag{3.35}$$

The second term in Eq. 3.31 is ZWD. The ZWD can also be integrated after specifying suitable relationships for temperature and water vapor pressure with height. Unfortunately, water vapor is rarely in hydrostatic equilibrium and varies significantly throughout the troposphere; hence, specifying an accurate relationship with height is difficult. However, it is common in meteorology to model the average decrease of water vapor (or total pressure) with height as an exponential function with exponent γ. From Smith (1966), the mixing ratio (w) of water vapor to moist air has been given approximately by

$$w = w_0 \left(\frac{P}{P_0} \right)^{\gamma} \tag{3.36}$$

where the zero subscript indicate surface (i.e., MSL) value. However, $w = (M_w/M)(e_s/P)$, $w_0 = (M_w/M)(e_0/P_0)$ and by substitution and re-arrangement, we can obtain:

$$e_s = e_0 \left(\frac{P}{P_0} \right)^{\gamma+1} \tag{3.37}$$

This provides a relationship for the average decrease in water vapor pressure with height. Separating the two ZWD components in Eq. 3.32 and ignoring the wet compressibility factors we have

$$\mathrm{ZWD} = 10^{-6} k_2' \int_{r_0}^{r_1} \frac{P_w}{T_K} \mathrm{d}r + 10^{-6} k_3 \int_{r_0}^{r_1} \frac{P_w}{T_K^2} \mathrm{d}r \tag{3.38}$$

By specifying a linear lapse rate (positive), β for temperature, the temperature throughout the troposphere can be represented as

$$T = T_0 \left(\frac{P}{P_0} \right)^{\frac{R_d \beta}{g}} \tag{3.39}$$

Combined with Eq. 3.35, allows for integration of Eq. 3.38. The formulation given by Askne and Nordius (1987) for ZWD is

$$\mathrm{ZWD} = \frac{10^{-6} k_2' R_d}{g_m(\gamma+1)} P_w + \frac{10^{-6} k_3 R_d}{g_m(\gamma+1-\beta R_d/g_m)} \frac{P_w}{T_K} \tag{3.40}$$

where the mean temperature of the water vapor $T_m = T\left(1 - \frac{\beta R_d}{g_m(\gamma+1)}\right)$ units of Kelvin. By using the models in Eqs. 3.35 and 3.41, a general formulation for the ZTD is found as

$$\mathrm{ZTD} = 10^{-6} k_1 \frac{R_d}{g_m} P + 10^{-6} \frac{R_d}{g_m} \left(\frac{k_2'}{(\gamma+1)} + \frac{k_3}{(\gamma+1-\beta R_d/g_m) T_K} \right) P_w \tag{3.41}$$

The ZTD model from Eq. 3.41 assumes that the delay caused by the ray bending and horizontal layer atmospheres is neglected. In general, because of a radio signal can come from slant directions, Saastamoinen (1972) and Hopfield (1969) develop a ZTD model by including slant delays (or slant tropospheric delay, STD) and internally cover a mapping function.

To derive of the ZTD model from Saastamoinen, we start with a truncated Taylor expansion of sec z in Fig. 3.3:

$$\sec z = \sec z_0 + \sec z_0 \tan z_0 \Delta z = \sec z_0 (1 + \tan z_0 \Delta z) \tag{3.42}$$

where, $\Delta z = z - z_0 = -\theta$ and $\tan z = r_0 \theta / (r - R_E)$. So by approximating $\tan z \approx \tan z_0$, Eq. 3.42 becomes

$$\sec z = \sec z_0 \left(1 - \tan^2 z_0 \frac{r - R_E}{R_E} \right) \tag{3.43}$$

with this expression, the STD reads

$$\mathrm{STD} = 10^{-6} \int_{R_E}^{\infty} N \sec z \, dr \tag{3.44}$$

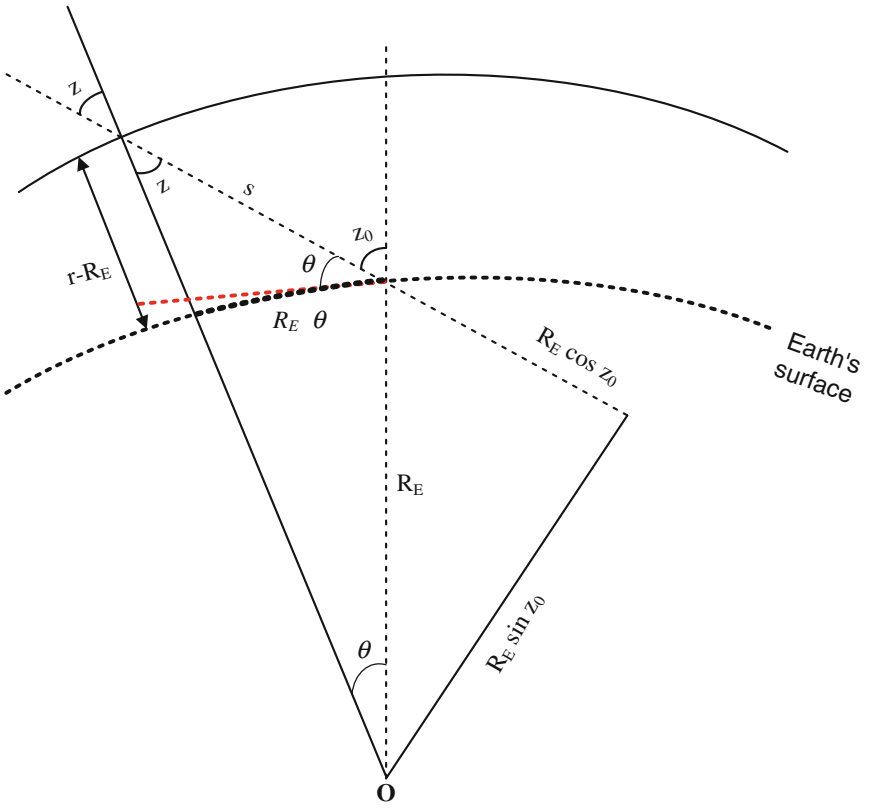

Fig. 3.3 Geometry of a ray arriving through a spherical atmosphere

$$= 10^{-6} \sec z_0 \left[\int_{R_E}^{\infty} N \, \mathrm{d}r - R_E^{-1} \tan^2 z_0 \int_{R_E}^{\infty} N(r - R_E) \mathrm{d}r \right] \tag{3.45}$$

The first term between the brackets in Eq. 3.45 is the zenith delay. The second term is a correction term of which the integral part can be subdivided into three sub-integrals

$$\int_{R_E}^{\infty} N \cdot (r - R_E) \mathrm{d}r = \underbrace{\int_{R_E}^{r_T} N \cdot (r - R_E) \mathrm{d}r}_{1} + \underbrace{\int_{r_T}^{\infty} N \cdot (r - r_T) \mathrm{d}r}_{2} + \underbrace{(r_T - R_E) \int_{r_T}^{\infty} N \, \mathrm{d}r}_{3} \tag{3.46}$$

where r_T is the radius of the tropopause, S is the traveled distance through the atmosphere, R_E is the radius of the Earth, z is the zenith angle at the top of the atmosphere, and z_0 is the zenith angle at the surface. Saastamoinen assumed the neutral atmosphere to consist of only two layers: the troposphere and the stratosphere. In this model, the troposphere is a polytrophic layer reaching up to r_T and the stratosphere is an isothermal layer, which for practical integration can be considered infinitely high. Each of the three integrals can be evaluated based on the refractivity profiles associated with the temperature profile.

The following evaluate of the integrals of Eq. 3.46, where Saastamoinen obtained his zenith delay model. In the troposphere, the temperature decreases with altitude. From this, the derivation of a pressure profile based on dry air we have differential equation

$$\frac{\mathrm{d}P}{P_d} = -\frac{g_m}{R_d T} \mathrm{d}h \tag{3.47}$$

The gravitation to be constant with height and equal to a mean value is considered.

$$g_m = \frac{\int_{h_0}^{\infty} \rho_m(h) g(h) \mathrm{d}h}{\int_{h_0}^{\infty} \rho_m(h) \mathrm{d}h} \tag{3.48}$$

For isothermal layer like the tropopause, the pressure profile is found by integration of Eq. 3.47

$$P_d = P_{d0} \exp\left(-\frac{h - h_0}{H} \right); \quad H = \frac{R_d T}{g_m} \tag{3.49}$$

In case of polytrophic layers, like the troposphere and stratosphere, the temperature lapse rate ($\beta = -\mathrm{d}T/\mathrm{d}H$) is assumed linear with height (H). We integrate the right-hand side of Eq. 3.48 over dT,

$$P_\mathrm{d} = P_{\mathrm{d}0} \exp\left(-\frac{T}{T_0}\right)^{\mu+1}; \quad \mu = \frac{g_\mathrm{m}}{R_\mathrm{d}\beta} - 1 \tag{3.50}$$

From Eqs. 3.12, 3.49, and 3.50, the refractivity profile of dry air can also be derived. For polytrophic layers

$$\frac{N_\mathrm{d}}{N_{\mathrm{d}0}} = \frac{k_1 P_\mathrm{d}/T}{k_1 P_{\mathrm{d}0}/T_0} = \left(\frac{T}{T_0}\right)^{\mu}; \quad \mu = -1 \tag{3.51}$$

In an isothermal layer ($T = T_0$) we find

$$\frac{N_\mathrm{d}}{N_{\mathrm{d}0}} = \frac{P_\mathrm{d}}{P_{\mathrm{d}0}} = \exp\left(-\frac{h - h_0}{H}\right) \tag{3.52}$$

where $P_{\mathrm{d}0}$ is the pressure of dry air at the surface of the layer (mbar), $N_{\mathrm{d}0}$ is the dry refractivity at the surface of the layer, T_0 is the temperature at the surface of the layer (K), h_0 is the height above MSL at the surface of the layer (km), h is the height above MSL (km), and H is the scale height in km ($H = r - R_\mathrm{E}$, see Fig. 3.3).

For the first integral in Eq. 3.48

$$N = N_0\left(\frac{T}{T_0}\right)^{\mu} \text{ and } \mathrm{T} = \mathrm{T}_0 - \beta\mathrm{H} \Rightarrow \begin{cases} H = -\left(\frac{T_0}{\beta}\right)\left(\frac{T}{T_0} - 1\right); \\ \frac{\mathrm{d}H}{\mathrm{d}T} = -\frac{1}{\beta} \end{cases} \tag{3.53}$$

After some straightforward computations, this results in

$$\begin{aligned} \int_{R_\mathrm{E}}^{\infty} N \cdot (r - R_\mathrm{E})\mathrm{d}r &= \int_{T_0}^{T_\mathrm{T}} N_0\left(\frac{T}{T_0}\right)^{\mu}\left(-\frac{T}{\beta}\right)\left(\frac{T}{T_0} - 1\right)\frac{1}{\beta}\mathrm{d}T \\ &= \frac{R_d}{g_\mathrm{m}^2(1 - R_\mathrm{d}\beta/g_\mathrm{m})}\left[N_0 T_0^2 - N_\mathrm{T} T_\mathrm{T}^2\right] \\ &\quad - \frac{R_\mathrm{d}}{g_\mathrm{m}}(r_\mathrm{T} - R_\mathrm{E}) N_\mathrm{T} T_\mathrm{T} \end{aligned} \tag{3.54}$$

where N_0 is the refractivity at Earth's surface (the index T stands for values at the tropopause), T_0 is the temperature at surface (or antenna) height (°C), β is the temperature lapse rate (0.0062 K km^{-1}), μ_m is the constant, $\mu_\mathrm{m} = \frac{g_\mathrm{m}}{R_\mathrm{d}\beta} - 1$, and g_m is the mean acceleration gravity (9.784 ms^{-2}).

The second integral, can be evaluated by using the assumption of an exponential profile of Eq. 3.52 and effective height (H_m)

$$N = N_T \exp\left(-\frac{r - r_T}{H}\right); \quad H_m = \frac{R_d T_T}{g_m} \tag{3.55}$$

and results in

$$\int_{r_T}^{\infty} N(r - r_T)\mathrm{d}r = \left(\frac{R_d}{g_m}\right)^2 N_T T_T^2 \tag{3.56}$$

The third integral is similar to Eq. 3.46 and results in

$$(r_T - R_E)\int_{r_T}^{\infty} N\mathrm{d}r = (r_T - R_E)10^{-6}k_1\frac{R_d}{g_m}P_T = \frac{R_d}{g_m}(r_T - R_E)N_T T_T \tag{3.57}$$

Summation of the three integral gives the total integral

$$\int_{R_E}^{\infty} N\,(r - r_T)\,\mathrm{d}r = \left(\frac{R_d}{g_m}\right)^2\left[\frac{N_0\,T_0^2 - \left(R_d\beta/g_m^2\right)N_T\,T_T^2}{1 - R_d\beta/g_m}\right] \tag{3.58}$$

With Eq. 3.31, the total Saastamoinen model then becomes

$$\begin{aligned} \mathrm{ZTD_{SAAS}} &= 10^{-6}\sec z_0\left[\int_{R_E}^{\infty} N\,\mathrm{d}r - R_E^{-1}\tan^2 z_0 \cdot \int_{R_E}^{\infty} N(r - R_E)\mathrm{d}r\right] \Rightarrow \\ \mathrm{ZTD_{SAAS}} &= 10^{-6}k_1\frac{R_d}{g_m}\sec z_0\left[P + \left(\frac{1255}{T_K} + 0.05\right)e_s - B(r)\tan^2 z_0\right] \end{aligned} \tag{3.59}$$

where

$$B(r) = \frac{1}{R_E}\frac{g_m}{R_d}\frac{1}{k_1}\int_{r_0}^{\infty} N(r - R_E)\,\mathrm{d}r \tag{3.60}$$

Tabular values for the correction term $B(r)$ are given by Saastamoinen (1972). The correction terms δR and $B(r)$ can be interpolated from Table 3.2. Saastamoinen did not mention the exact theoretical standard atmosphere he used to find the tabular values of $B(r)$. However, the standard values at MSL as also later used in the 1976 US Standard Atmosphere (T_{MSL} = 288.15 K, P_{MSL} = 1013.25 mbar), as well as the

Table 3.2 Correction terms for Saastamoinen neutral delay model (Hofmann-Wellenhof et al. 2001)

Zenith distance	Station height above sea level (km)							
	0	0.5	1	1.5	2	3	4	5
60°00′	0.003	0.003	0.002	0.002	0.002	0.002	0.001	0.001
66°00′	0.006	0.006	0.005	0.005	0.004	0.003	0.003	0.002
70°00′	0.012	0.011	0.010	0.009	0.008	0.006	0.005	0.004
73°00′	0.020	0.018	0.017	0.015	0.013	0.011	0.009	0.007
75°00′	0.031	0.028	0.025	0.023	0.021	0.017	0.014	0.011
76°00′	0.039	0.035	0.032	0.029	0.026	0.021	0.017	0.014
δR, m: 70°00′	0.050	0.045	0.041	0.037	0.033	0.027	0.022	0.018
78°00′	0.065	0.059	0.054	0.049	0.044	0.036	0.030	0.024
78°30′	0.075	0.068	0.062	0.056	0.051	0.042	0.034	0.028
79°00′	0.087	0.079	0.072	0.065	0.059	0.049	0.040	0.033
79°30′	0.102	0.093	0.085	0.077	0.070	0.058	0.047	0.039
79°45′	0.111	0.101	0.092	0.083	0.076	0.063	0.052	0.043
80°00′	0.121	0.110	0.100	0.091	0.083	0.068	0.056	0.047
B(r), mbar	0.156	1.079	1.006	0.938	0.874	0.757	0.654	0.563

values $r_0 = 6360$ km and $h_T = 15$ km, fit quite well. A slightly different table for the $B(r)$ values can be found in Saastamoinen (1972).

The ZTD of Saastamoinen model has refined his model by adding an additional term is used to account for the delay caused by the ray bending, δR as a complete form:

$$\mathrm{ZTD_{SAAS}} = 10^{-6} k_1 \frac{R_\mathrm{d}}{g_\mathrm{m}} \sec z_0 \left[P + \left(\frac{1255}{T_\mathrm{K}} + 0.05 \right) P_\mathrm{w} - B(r) \tan^2 z_0 \right] + \delta R \tag{3.61}$$

where k_1 is the hydrostatic refractivity constant ($k_1 = 77.6 \pm 0.05$ K mbar^{-1}), $B(r)$ is the correction term of height dependent (mbar), δR is the correction term of ray bending (m), and z_0 is the zenith distance of the satellite or apparent zenith angle $z_0 = 90° - \theta$.

Looked at the first term in Eq. 3.61, the ZHD is with a mapping function sec z_0. The mean gravitational acceleration depends on latitude and height of the antenna. Based on Saastamoinen (1972) approximation, the weighted mean gravity (g_m) is used to correct the gravitational acceleration at the center of mass of the vertical atmospheric column directly above the station depends on height at site and geodetic latitude, and is given as follows (Davis et al. 1985):

$$g_\mathrm{m} = 9.784\, f(\varphi, h) \tag{3.62}$$

Finally, the expression for ZHD from Saastamoinen can be written as follows:

$$\mathrm{ZHD}_{\mathrm{SAAS}}(P,\varphi,h) = (2.2768 \pm 0.0024)\frac{P}{f(\varphi,h)} \tag{3.63}$$

where $f(\varphi,h) = 1 - 0.00266\cos(2\varphi) - 0.00028h$, is the correction factor for the local gravitational acceleration, φ is the site latitude (in degrees) and h is the height of the site above the ellipsoid (in km). Accurately, with Eq. 3.63, for any location on Earth, when the surface pressure is given, the ZHD value can be computed.

From the second term in the bracket of Eq. 3.61, Saastamoinen (1972) determine the ZWD with an assumption that the partial pressure water vapor and temperature were decreased linearly with height. The final expression of ZWD is

$$\mathrm{ZWD}_{\mathrm{SAAS}} = 0.002277\left(\frac{1225}{T_{\mathrm{s}}} + 0.05\right)P_{\mathrm{w}} \tag{3.64}$$

where T_{s} is the surface temperature in °C and P_{w} is the partial water vapor in mbar.

3.3.2 The Hopfield Model

Hopfield (1969) developed a dual quartic zenith model of the refractivity with different quartics for the dry and wet atmospheric profiles using real data of surface measurements (pressure, temperature, and humidity) covering the whole Earth. This model assumes that the atmosphere is in hydrostatic equilibrium, which follows from the ideal gas law. The model also assumes the acceleration due to gravity and lapse rate in temperature is constant with height derived from a least-square fit to collected data. The model expresses the total delay in terms up to the fourth power of the refractive index. A representation of the dry and wet refractivity can be written as a function of height h above the surface by

$$N_j^{\mathrm{Trop}}(h) = N_{j,0}^{\mathrm{Trop}}\left(1 - \frac{h}{h_j}\right)^4 \tag{3.65}$$

with total refractivity at surface of the Earth given as

$$N_{j,0}^{\mathrm{Trop}} = N_{\mathrm{d},0}^{\mathrm{Trop}} + N_{\mathrm{w},0}^{\mathrm{Trop}} = \underbrace{k_1\frac{P}{T_{\mathrm{K}}}}_{\text{dry}} + \underbrace{k_2\frac{P_{\mathrm{w}}}{T_{\mathrm{K}}} + k_3\frac{P_{\mathrm{w}}}{T_{\mathrm{K}}^2}}_{\text{wet}} \tag{3.66}$$

where j is the subscript for dry component (replace j by d) and wet component (replace j by w). N_j^{Trop} is the refractivity above the Earth surface, $N_{j,0}^{\mathrm{Trop}}$ is the refractivity at the surface of the Earth, k_2 and k_3 are refraction constants

($k_2 = -12.96$ K mbar^{-1} and $k_3 = 5.718 \times 10^5$ K^2 mbar^{-1}), and h_j are the hydrostatic and wet thickness of atmospheric layer (m), respectively.

It assumes the atmosphere is a single polytrophic layer, thickness h_d was obtained by using global radiosonde data (Hofmann-Wellenhof et al. 2001):

$$h_d = 40{,}136 + 148.72\, T_K \tag{3.67}$$

Unique values for h_d cannot be given because they depend on location and temperature. Figure 3.4 shows the thickness of polytrophic layers for the tropospheric. The effective troposphere heights are given as 40 km ≤ h_d ≤ 45 km and 10 km ≤ h_w ≤ 13 km for dry and wet components, respectively. The effective height for the wet component h_w is usually set to a default value of 11 km. Alternatively, Mendes and Langley (1998) found the relation between the surface temperature and the tropopause height denoted as H_T (in meters),

$$h_w = H_T = 7{,}508 + 0.002421 \exp\left(\frac{T}{22.90}\right) \tag{3.68}$$

Referring to Fig. 3.4, substitution of Eqs. 3.66 and 3.67 into the general Eq. 3.30 for the tropospheric path delay (ZPD) yields

$$\mathrm{ZPD} = 10^{-6} N_{j,0}^{\mathrm{Trop}} \int \left(1 - \frac{h}{h_j}\right)^4 \mathrm{d}s \tag{3.69}$$

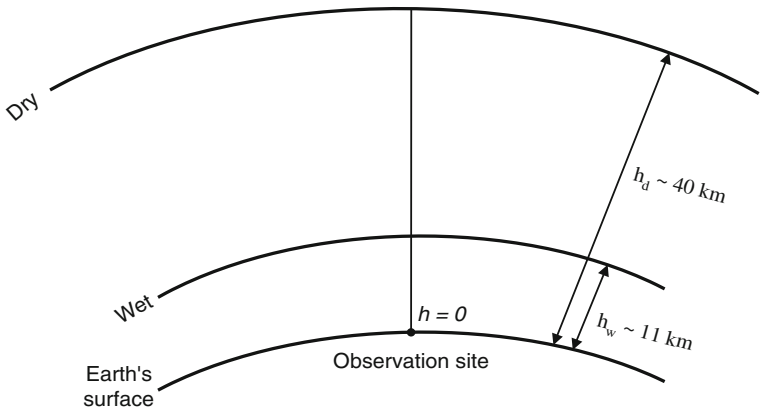

Fig. 3.4 Thickness of polytrophic layers for the troposphere adapted from Hofmann-Wellenhof et al. (2001)

The integral can be solved if the delay is calculated along the vertical direction and if the curvature of the signal path is neglected. Extracting the constant denominator, Eq. 3.69 becomes

$$\mathrm{ZPD} = 10^{-6} N_{j,0}^{\mathrm{Trop}} \frac{1}{h_j^4} \int_{h=0}^{h=h_j} \left(h_j - h\right)^4 \mathrm{d}h \tag{3.70}$$

For an observation site on the Earth's surface (i.e., $h = h_s$) and after integration,

$$\mathrm{ZPD} = 10^{-6} N_{j,0}^{\mathrm{Trop}} \frac{1}{h_j^4} \left[-\frac{1}{5} \left(h_j - h\right)^5 \middle| \begin{matrix} h = h_j \\ h = h_s \end{matrix} \right] \tag{3.71}$$

The evaluation of the expression between the brackets gives the ZPD as follows:

$$\mathrm{ZPD} = \frac{10^{-12}}{5} N_{j,0}^{\mathrm{Trop}} \frac{1}{h_j^4} \left(h_j - h_s\right)^5 \tag{3.72}$$

where h_s is the height position of the receiver at site (in meters). If $h_s = 0$ as shown in Fig. 3.4, Eq. 3.72 can be rewritten as given by Hofmann-Wellenhof et al. (2001) and separating the hydrostatic and wet components, the total ZPD (in meters) is

$$\mathrm{ZPD} = \frac{10^{-12}}{5} N_{j,0}^{\mathrm{Trop}} h_j = \frac{10^{-6}}{5} \left[N_{\mathrm{d},0}^{\mathrm{Trop}} h_{\mathrm{d}} + N_{\mathrm{w},0}^{\mathrm{Trop}} h_{\mathrm{w}} \right] \tag{3.73}$$

The model in its present form does not account for an arbitrary elevation angle of the signal. Considering the line of sight, an obliquity factor must be applied for projecting the dependence of the zenith delays to the slant direction as a mapping function. Therefore, a slight variation of the Hopfield model contains an arbitrary elevation angle θ at the observation site using $1/\sin\left(\theta^2 + 6.25\right)^{1/2}$ as a mapping function for the hydrostatic component and $1/\sin\left(\theta^2 + 2.25\right)^{1/2}$ for the wet component. Hence, the total tropospheric delay at a zenith can be written as follows

$$\mathrm{ZTD}_{\mathrm{HOP}}(\theta) = \mathrm{ZHD}_{\mathrm{HOP}}(\theta) + \mathrm{ZWD}_{\mathrm{HOP}}(\theta) \tag{3.74}$$

where

$$\mathrm{ZHD}_{\mathrm{HOP}}(\theta) = \frac{10^{-6}}{5} \frac{77.64 \frac{P}{T_{\mathrm{K}}}}{\sin \sqrt{\left(\theta^2 + 6.25\right)}} h_{\mathrm{d}} \tag{3.75}$$

$$\mathrm{ZWD}_{\mathrm{HOP}}(\theta) = \frac{10^{-6}}{5} \frac{\left(-12.96 T_{\mathrm{K}}\right) + 3.718 \times 10^5}{\sin \sqrt{\left(\theta^2 + 2.25\right)}} \left(\frac{e_s}{T_{\mathrm{K}}^2} \right) h_{\mathrm{w}} \tag{3.76}$$

3.3.3 The Modified Hopfield Model

The reference of station height on the Earth surface is inaccurate because of the terrestrial points to be referred to a global frame. To overcome this limitation, the atmospheric layer is considered to have azimuthally symmetry in ZTD estimation. Therefore, the modified Hopfield model (Hofmann-Wellenhof et al. 2001) is refined introducing the lengths of position vectors instead of height to correct the Hopfield model for the determination of refractivity and denoting the earth's radius by R_E, the corresponding lengths are $r_{hyd} = R_E + h_{hyd}$ and $r = R_E + h_{wet}$ as shown in Fig. 3.5. R_E is taken as 6,378,137 meters in this paper. The empirical representation of refractivity to the Modified Hopfield model, N_j as a function of height h above the surface can be written as (Hofmann-Wellenhof et al. 2001),

$$N_j^{\text{Trop}}(r) = N_{j,0}^{\text{Trop}} \left(\frac{r_j - r}{r_j - R_E} \right)^4 \tag{3.77}$$

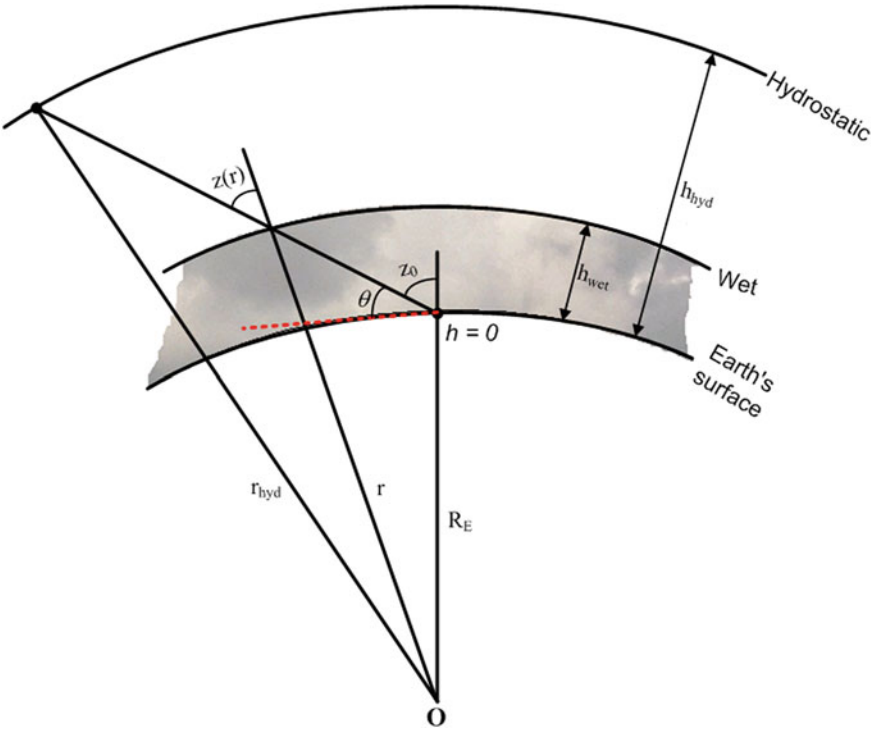

Fig. 3.5 Geometry for tropospheric path delay based on modified Hopfield model is adapted from Hofmann-Wellenhof et al. (2001)

where for the hydrostatic refractivity component subscript j is replaced by hyd and for the wet refractivity component subscript j is replaced by wet, respectively. In the equation, N_j^{Trop} represent the refractivity above the earth surface and $N_{j,0}^{\text{Trop}}$ is the refractivity at the surface of the earth.

In this work, we corrected the refractivity by taking the dry $\left(Z_{\text{dry}}^{-1}\right)$ and wet $\left(Z_{\text{wet}}^{-1}\right)$ inverse compressibility factors into account for the determination of $N_{j,0}^{\text{Trop}}$ assuming that a nonideal gas represents the neutral atmosphere layer. Both the formula for Z_{dry}^{-1} and Z_{wet}^{-1} have been determined empirically by Owens (1967) as shown in Eqs. 3.6 and 3.7. By applying the ideal gas equation of state to the dry refractivity component in the Thayer equation (1974), $N_{\text{dry}} = k_1\left(P_{\text{dry}}/T_{\text{K}}\right)Z_{\text{dry}}^{-1}$, the dry inverse compressibility factor $\left(Z_{\text{dry}}^{-1}\right)$ is eliminated and this term is changed to the hydrostatic term, $N_{\text{hyd}} = k_1(P/T_{\text{K}})$. The refraction constant k_2 in the wet term of Eq. 3.66 is also corrected with a new constant k_2' as shown in Eq. 3.17. The total refractivity at the surface of the earth is then given as

$$N_{j,0}^{\text{Trop}} = N_{\text{hyd},0}^{\text{Trop}} + N_{\text{wet},0}^{\text{Trop}} = \underbrace{k_1\frac{P}{T_{\text{K}}}}_{\text{hydrostatic}} + \underbrace{\left(\underbrace{k_2'\frac{P_{\text{wet}}}{T_{\text{K}}}Z_{\text{wet}}^{-1}}_{\text{dipole moment}} + \underbrace{k_3\frac{P_{\text{wet}}}{T_{\text{K}}^2}Z_{\text{wet}}^{-1}}_{\text{dipole orientation}}\right)}_{\text{wet}} \tag{3.78}$$

where in the first term is hydrostatic refractivity in equilibrium state and the last term is the wet refractivity component. In Eq. 3.78 the 'dry' term has been replaced by 'hydrostatic' term.

Taking Eq. 3.78 for the hydrostatic delay and introducing mapping function $(1/\cos z)$, where zenith angle, $z(r) = 90^\circ - \theta(r)$ is a variable and θ is the elevation angle at the observation site as shown in Fig. 3.5, the ZHD after applying the sine law can be expressed as

$$\text{ZHD} = \frac{10^{-6}N_{\text{hyd},0}^{\text{Trop}}}{\left(r_{\text{hyd}} - R_{\text{E}}\right)^4}\int_{r=R_{\text{E}}}^{r=r_{\text{d}}}\frac{r\left(r_{\text{hyd}} - r\right)^4}{\sqrt{r^2 - a^2}}\text{d}r \tag{3.79}$$

where the terms in the integral are constant except for r which is variable and $a = R_{\text{E}}\cos\theta$. Assuming the same model for the wet component, the corresponding formula is given by

$$\text{ZWD} = \frac{10^{-6}N_{\text{wet},0}^{\text{Trop}}}{\left(r_{\text{wet}} - R_{\text{E}}\right)^4}\int_{r=R_{\text{E}}}^{r=r_{\text{w}}}\frac{r\left(r_{\text{wet}} - r\right)^4}{\sqrt{r^2 - a^2}}\text{d}r \tag{3.80}$$

The integral in both equations can be solved by a series expansion of the integrand. Adopting the series expansion of Goad and Goodman (as cited in Hofmann-Wellenhof et al. 2001) the solution to the integral r_j is given as follows:

$$r_j = \left[R_E^2\left(1+\frac{h_j}{R_E}\right)^2 - a^2\right]^{1/2} - \left[R_E^2 - a^2\right]^{1/2} \tag{3.81}$$

Solutions of the total ZTD (in meters) as a function of θ, P, T, and H from Eqs. 3.79 and 3.80 can be expressed as (Suparta et al. 2008)

$$\mathrm{ZTD} = 10^{-6} N_{j,0}^{\mathrm{Trop}} \begin{bmatrix} 1 + 4a_j \frac{r_j^2}{2} + \left(6a_j^2 + 4b_j\right)\frac{r_j^3}{3} + 4a_j\left(a_j^2 + 3b_j\right)\frac{r_j^4}{4} \\ + \cdots \left(a_j^4 + 12a_j^2 b_j + 6b_j^2\right)\frac{r_j^5}{5} + 4a_j b_j\left(a_j^2 + 3b_j\right)\frac{r_j^6}{6} \\ + \cdots b_j^2\left(6a_j^2 + 4b_j\right)\frac{r_j^7}{7} + 4a_j b_j^3 \frac{r_j^8}{8} + b_j^4 \frac{r_j^9}{9} \end{bmatrix} \tag{3.82}$$

$$a_j = -\frac{\sin\theta}{h_j} \quad \text{and} \quad b_j = -\frac{\cos^2\theta}{2h_j R_E} \tag{3.83}$$

In general, Eq. 3.82 can be written as (Hofmann-Wellenhof et al. 2001)

$$\mathrm{ZTD}(\theta, P, T, H) = 10^{-6} N_j^{\mathrm{Trop}} \left(\sum_{k=1}^{9} \frac{\alpha_{k,j}}{k} r_j^k\right) \tag{3.84}$$

In Eqs. 3.82 and 3.83, the factor of 10^{-6} was corrected from 10^{-12} in Hofmann-Wellenhof et al. (2001: 115) to meet a consistency solution from Eqs. 3.79 and 3.80. In Eq. 3.83, h_j (in meters) represent h_{hyd} and h_{wet} are the effective height for the hydrostatic and wet components, respectively. In this work, h_{h} in Eq. 3.67 is used and the tropopause height or wet component (h_{wet}) is set to 11 km. The elevation angle is extracted from the GPS signals. In Eq. 3.84, k is the tropospheric layer.

Comparing the ZTD accuracies for both Hopfield and Saastamoinen models, the standard deviations of both models have very small difference of about 0.2 and 12.4 mm for the hydrostatic and wet components, respectively. Note that unlike the Hopfield and Saastamoinen models described earlier for the zenith delay, the Modified Hopfield model is also introduced for slant delays.

3.4 The Mapping Function

A mapping function is defined as the ratio of the electrical path length (also referred to as the delay) through the atmosphere at a geometric elevation, to the electrical path length in the zenith direction (Niell 2000). It is developed due to the tropospheric delay is the shortest in the zenith direction and becomes larger with increasing zenith angle. For GPS measurement of zenith PWV, the signal delay in each direction to each GPS satellite is not generally estimated individually. Instead, the individual delays are mapped from each individual satellite direction to a single zenith delay. This mapping method assumes that the delay is independent of azimuth. This assumption could never be made because of the significant increase in delay that is seen when the signal travels through much more of the atmosphere at lower elevations. Mapping functions account for the delay for individual satellite view and map them to the zenith direction.

Similar to the tropospheric models, many mapping functions have been proposed, such as Black (1978), Baby et al. (1988), Chao (1972), Davis et al. (1985), Herring (1992), Hopfield (1969), and Niell (1996). However, three mapping functions above are widely used because it included the hydrostatic and wet mapping functions. Those models of Davis, Herring, and Niell are called CfA-2.2 (Harvard–Smithsonian Center of Astrophysics), MTT (Massachusetts Institute of Technology, MIT Haystack Observatory), and new mapping functions, respectively. The CfA-2.2 mapping function (Davis et al. 1985) was designed to achieve sub-centimeter accuracy at 5 degrees elevations. The MTT mapping function (Herring 1992) can be used to represent the elevation angle dependence of the tropospheric delay with an RMS of less than 0.2 mm for elevation angles larger than 3 degrees. The last one is the new global mapping function by Niell (1996), namely the Niell Mapping Function (NMF). The NMF mapping functions almost similar to the MTT, which can be used for elevation angles down to 3 degrees.

Nowadays, the NMF mapping derived from Very Long Base Interferometry (VLBI) observations is the most widely used and known to be most accurate and easily implemented functions. Niell (1996) recognized that mapping functions like those of CfA-2.2, MTT, and Ifadis (1992) which all depend on surface temperatures. Unfortunately, the temperatures are much more variable in particular at higher altitudes both diurnally and on longer time scales, resulting in an error in the mapping. Therefore, NMF was developed to be independent of surface meteorological parameters. In this section, a simplest (cosecant) mapping function is introduced, then the Niell mapping function. The selection of this functional model is based on its ability to perform well in both low and high elevation and its independence meteorological parameters (Leick 1995).

3.4.1 The Cosecant Mapping Function

Foelsche and Kirchengast (2001) introduce a simple "geometric" mapping function (Fig. 3.6), where only the free parameter is an "effective height" of the atmosphere, corresponding to about the first two scales height above the surface. The simplest mapping function is the cosecant of the elevation angle that assumes both the curvature of the earth and the curvature of the path of the GPS signal propagating through the atmosphere can be approximated as plane surfaces. This is a reasonably accurate approximation only for high elevation angles with a small degree of bending.

To simplify Fig. 3.6, the value of ds/dr is defined to be the ratio of the slant straight-line ray path length within the effective height, S_{atm} ($S_{\text{atm}} = s$) to the H_{atm} itself.

$$\mathrm{d}s/\mathrm{d}r = S_{\text{atm}}/H_{\text{atm}} \tag{3.85}$$

The above equation in other ways can be written in the form directly expressing the deviation from the simple cosecant law

$$\frac{\mathrm{d}s}{\mathrm{d}r} = \frac{1}{\cos z \, \frac{S_{\text{flat}}}{S_{\text{atm}}}} \tag{3.86}$$

where dr is the difference in radius (distance to the center of the Earth) of the two layers, ds is the distance difference, z is the zenith angle at an arbitrary layer, S_{flat}

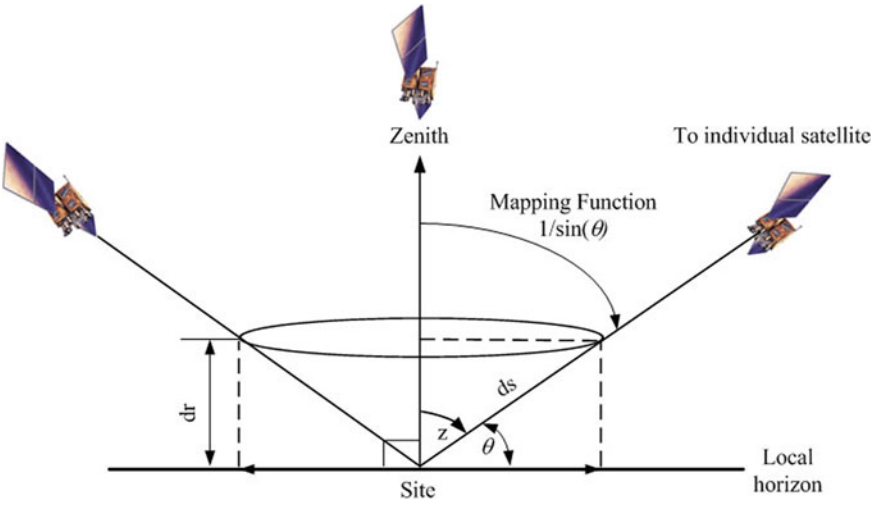

Fig. 3.6 Propagation of GPS signals approximated as a planar surface (Suparta 2008)

would be the ray path within H_{atm} in a flat (plane-parallel) atmosphere and ds/dr is the mapping function, later known as $m(z)$. Therefore, Eq. 3.86 is rewritten as

$$m(z) = \frac{1}{\cos z \frac{S_{\text{flat}}}{S_{\text{atm}}}} \tag{3.87}$$

For the planar atmosphere, assume that the Earth is flat and refractivity is constant, hence $S_{\text{atm}} \cong S_{\text{flat}}$. The cosecant mapping function becomes 1/sin (*elevation*). As can be seen in Fig. 3.6, for an infinitesimal thin layer we have

$$m(z) = \frac{1}{\cos z} \equiv \sec z \rightarrow m(\theta) = \frac{1}{\sin \theta} \tag{3.88}$$

Because of the curvature of the atmosphere, this zenith angle change along the ray path. A simple mapping function in Eq. 3.88 is limited for use above $\sim$60 degrees elevation. As the ratio of the thickness of the atmosphere to the radius of the earth decreases, the atmosphere appears more planar. This thickness varies with latitude and season. Thus, a possible proxy for the mapping function is some quantity that is a measure of the thickness of the atmosphere. The more complex mapping functions are based on the truncation of the continued fractions. This type of mapping functions includes Chao (1972), Davis et al. (1985), Marini (1972), and Niell (1996). The following is the description the Niell mapping function.

3.4.2 The Niell Mapping Function

Differing from most typical tropospheric delay models, Niell has developed hydrostatic and wet mapping functions with new forms and their combined use to reduce errors in geodetic estimation for observations as low as 3° in elevation. Although it has no parameterization in terms of actual meteorological conditions, they agree as well or better than mapping functions calculated from radiosonde profiles. In fact, when there is no information about the state of the atmosphere other than at the surface, the variation of the mapping function is found to be better modeled in terms of the seasonal dependence of the atmosphere, which is taken to be sinusoidal and in terms of the latitude and height above sea level of the site. The form adopted for this mapping function is the continued fraction of Marini (1972) with three constants but normalized to unity at the zenith as proposed by Herring (1992).

Marini (1972) was the first one to come up with the idea to use continued fractions. The most recent mapping functions are those of Herring (1992), Ifadis (1992), and Niell (1996), which used the continued fractions. Continued fractions have the advantage over models with Taylor's expansions like the Saastamoinen model because they fit for nearly the whole range of zenith angles (see Fig. 3.3).

The following is one type of the mapping function presented by Herring (1992) with continued fractions

$$M(z_0) = \frac{1 + a/(1 + b/(1 + c/(1 + \cdots)))}{a} \Big/ \left(\cos z_0 + \frac{b}{\cos z_0 + \frac{c}{\cos z_0 + \cdots}}\right) \tag{3.89}$$

where a, b, and c are mapping function coefficients to be determined. For low precision, the coefficients can be set to $a = b = c = 0$, which yields the cosecant model as introduced in Sect. 3.4.1.

Based on the continued fraction, Niell (1996) has developed hydrostatic and wet mapping functions with new forms and combinations. It is used to reduce errors in geodetic estimation to provide a better fit and give better accuracy over the latitude range 43° N to 75° N for observations down to 3 degrees elevation. The form adopted for Niell mapping function is the continued fraction of Marini (1972) with three a, b, and c constants in the following.

$$m_j(\theta) = \frac{\dfrac{1}{1 + \dfrac{a_j}{1 + \dfrac{b_j}{1 + c_j}}}}{\sin\theta + \dfrac{a_j}{\sin\theta + \dfrac{b_j}{\sin\theta + c_j}}} \tag{3.90}$$

In addition to a latitude and seasonal dependence due to varying solar radiation, the hydrostatic mapping function should also be dependent on the height above the geoid of the point of observation because the ratio of the atmosphere "thickness" to the radius of curvature decreases with height. This does not apply to the wet mapping function since the water vapor is not in hydrostatic equilibrium and the height distribution of the water vapor is not expected to be predictable from the station height. The Niell mapping function for the hydrostatic (replace j by hyd) and wet (replace j by wet) components is of the following form

$$m_j(\theta) = \underbrace{m_{\mathrm{h}}(\theta) + \Delta m(\theta)}_{\text{hydrostatic}} + m_{\mathrm{wet}}(\theta) \tag{3.91}$$

For the hydrostatic mapping function, Niell (1996) adjusted the heights above the geoid. The sensitivity of the hydrostatic mapping function to the height above MSL was determined by beginning the ray-trace with nine different elevation angles between 3 and 90 degrees to give both the hydrostatic and wet path delays of each of the nine standard profiles with the values of pressure, temperature, and relative humidity at 1 and 2 km altitude. The height correction, $\Delta m(\theta)$, is given by

$$\Delta m(\theta) = \frac{\mathrm{d}m(\theta)}{\mathrm{d}h} h \tag{3.92}$$

where h is the height of the site above geoid in meters. The analytic height correction coefficients is taken to be

$$\frac{\mathrm{d}m(\theta)}{\mathrm{d}h} = \Delta m(\theta) = \frac{1}{\sin\theta} - f(\theta, a_{\mathrm{ht}}, b_{\mathrm{ht}}, c_{\mathrm{ht}}) \tag{3.93}$$

Here, $f(\theta, a_{\mathrm{ht}}, b_{\mathrm{ht}}, c_{\mathrm{ht}})$ represents the three-term continued fraction expressed by Eq. 3.94 in the Marini mapping function,

$$f(\theta, a_{\mathrm{ht}}, b_{\mathrm{ht}}, c_{\mathrm{ht}}) = \frac{1 + (a_{\mathrm{ht}}/(1 + b_{\mathrm{ht}}/(1 + c_{\mathrm{ht}})))}{\sin\theta + (\sin\theta + a_{\mathrm{ht}}/(\sin\theta + b_{\mathrm{ht}}/(\sin\theta + b_{\mathrm{ht}})))} \tag{3.94}$$

In the above equation, the coefficients $a_{\mathrm{ht}} = 2.53 \times 10^{-5}$, $b_{\mathrm{ht}} = 5.49 \times 10^{-3}$, and $c_{\mathrm{ht}} = 1.14 \times 10^{-3}$ was determined by least-square fits to the height corrections at the nine elevation angles. In these fittings, Niell used one for north latitudes of 15° for the whole year and two for north latitudes of 30°, 45°, 60°, and 75°, for the months January and July as tabulated in Cole et al. (1965).

Finally, the hydrostatic mapping function has normalized to yield a value of unity at the zenith and with a height correction, $\Delta m(\theta)$, which can be written as

$$m_{\mathrm{hyd}}(\theta) = \frac{1 + (a/(1 + b/(1 + c)))}{\sin\theta + (a/\sin\theta + (b/\sin\theta + c))} + \left[\frac{1}{\sin\theta} - f(\theta, a_{\mathrm{ht}}, b_{\mathrm{ht}}, c_{\mathrm{ht}})\right] h \tag{3.95}$$

For Niell, wet mapping function can be written as

$$m_{\mathrm{wet}}(\theta) = \frac{1 + (a/(1 + b/(1 + c)))}{\sin\theta + (a/\sin\theta + (b/\sin\theta + c))} \tag{3.96}$$

The coefficients a, b, and c in Eq. 3.89 were derived from temperature and relative humidity profiles of the U.S. Standard Atmosphere which is dependent on the latitude at North regions 15° (tropical), 30° (subtropical), 45° (midlatitude), 60 and 75° (subarctic) for the months of January (Winter) and July (Summer) and takes seasonal variations into account. Niell assumes that the Southern and Northern hemispheres are antisymmetric in time, i.e., the seasonal behavior is the same. In addition, he assumes the equatorial region is described by the 15° N latitude profile while the polar region is described by the 75° N latitude profile.

For the hydrostatic component, these coefficients are determined based on height, latitude, and DoY (day of year). However, for the wet mapping function, they depend only on the latitude. The coefficients for hydrostatic mapping function can be interpolated based on the parameter values extracted from Table 3.3 by the following interpolation rule.

Table 3.3 Coefficients of the hydrostatic mapping function

Coefficient	$\varphi = 15°$	$\varphi = 30°$	$\varphi = 45°$	$\varphi = 60°$	$\varphi = 75°$
a_{avg}	1.2769934×10^{-3}	1.2683230×10^{-3}	1.2465397×10^{-3}	1.2196049×10^{-3}	1.2045996×10^{-3}
b_{avg}	2.9153695×10^{-3}	2.9152299×10^{-3}	2.9288445×10^{-3}	2.9022565×10^{-3}	2.9024912×10^{-3}
c_{avg}	62.610505×10^{-3}	62.837393×10^{-3}	63.721774×10^{-3}	63.824265×10^{-3}	64.258455×10^{-3}
a_{amp}	0.0	1.2709626×10^{-5}	2.6523662×10^{-5}	3.4000452×10^{-5}	4.1202191×10^{-5}
b_{amp}	0.0	2.1414979×10^{-5}	3.0160779×10^{-5}	7.2562722×10^{-5}	11.723375×10^{-5}
c_{amp}	0.0	9.0128400×10^{-5}	4.3497037×10^{-5}	84.795348×10^{-5}	170.37206×10^{-5}

For latitude $|\varphi| \leq 15^\circ$

$$F(\varphi, t) = F_{\text{avg}}(15^\circ) + F_{\text{amp}}(15^\circ) \cos\left(2\pi \frac{\text{DoY} - T_0}{365.25}\right) \tag{3.97}$$

For latitude range $15^\circ \leq |\varphi| \leq 75^\circ$,

$$\begin{aligned} F(\varphi, t) = {} & F_{\text{avg}}(\varphi_i) + \left[F_{\text{avg}}(\varphi_{i+1}) - F_{\text{avg}}(\varphi_i)\right] \frac{\varphi - \varphi_i}{\varphi_{i+1} - \varphi_i} \\ & + \cdots \left\{F_{\text{amp}}(\varphi_i) + \left[F_{\text{amp}}(\varphi_{i+1}) - F_{\text{amp}}(\varphi_i)\right] \frac{\varphi - \varphi_i}{\varphi_{i+1} - \varphi_i}\right\} \\ & \cos\left(2\pi \frac{\text{DoY} - T_0}{365.25}\right) \end{aligned} \tag{3.98}$$

For latitude $|\varphi| \geq 75^\circ$,

$$F(\lambda, t) = F_{\text{avg}}(75^\circ) + F_{\text{amp}}(75^\circ) \cos\left(2\pi \frac{\text{DoY} - T_0}{365.25}\right) \tag{3.99}$$

where φ is the user's latitude and the subscripts refer to the nearest tabular latitude, F is the mapping function calculated coefficients a, b, and c, separated into average values and amplitudes. T_0 is the day of a year for "maximum winter" which is set to 28 for Northern Hemisphere and 211 for the Southern Hemisphere. The average and amplitude values of the hydrostatic mapping function coefficients are listed in Table 3.3.

For the latitude $|\varphi| \leq 15^\circ$,

$$F(\varphi, t) = F_{\text{avg}}(15^\circ) + F_{\text{amp}}(15^\circ) \cdot \cos\left(2\pi \frac{\text{DoY} - T_0}{365.25}\right) \tag{3.100}$$

For the latitude $|\varphi| \geq 75^\circ$,

$$F(\lambda, t) = F_{\text{avg}}(75^\circ) + F_{\text{amp}}(75^\circ) \cdot \cos\left(2\pi \frac{\text{DoY} - T_0}{365.25}\right) \tag{3.101}$$

In case of the wet mapping function, the interpolation rule is also following the equation, but the average values for a_{wet}, b_{wet}, and c_{wet} are shown in Table 3.4.

For the latitude $|\varphi| \leq 15^\circ$,

$$F(\varphi, t) = F_{\text{avg}}(15^\circ) \tag{3.102}$$

Table 3.4 Coefficients of the wet mapping function

Coefficient	$\varphi = 15°$	$\varphi = 30°$	$\varphi = 45°$	$\varphi = 60°$	$\varphi = 75°$
a_{avg}	5.8021879×10^{-4}	5.6794847×10^{-4}	5.8118019×10^{-4}	5.9727542×10^{-4}	6.1641693×10^{-4}
b_{avg}	1.4275268×10^{-3}	1.5138625×10^{-3}	1.4572752×10^{-3}	1.5007428×10^{-3}	1.7599082×10^{-3}
c_{avg}	4.3472961×10^{-2}	4.6729510×10^{-2}	4.3908931×10^{-2}	4.4626982×10^{-2}	5.4736039×10^{-2}

For the latitude range $15^\circ \leq |\varphi| \leq 75^\circ$,

$$F(\varphi, t) = F_{\text{avg}}(\varphi_i) + \left[F_{\text{avg}}(\varphi_{i+1}) - F_{\text{avg}}(\varphi_i)\right] \cdot \frac{\varphi - \varphi_i}{\varphi_{i+1} - \varphi_i} \tag{3.103}$$

For the latitude $|\varphi| \geq 75^\circ$,

$$F(\varphi, t) = F_{\text{avg}}(75^\circ) \tag{3.104}$$

Conclusively, Tables 3.3 and 3.4 show the dependency of coefficients *a*, *b,* and *c* on temporal and spatial conditions for hydrostatic and wet mapping functions, respectively. To use the mapping function for any latitude, linear interpolation between the coefficients is required. Above 75° the same coefficients may be used as those at 75°. Between 15° N and 15° S, the coefficients may be considered constant. On this basis, the NMF mapping functions were estimated to be error by less than 4 mm from 12° down to 3° in comparison to the MTT mapping functions of Herring, but with smaller biases relative to ray traces than the MTT mapping functions.

References

Askne J, Nordius H (1987) Estimation of tropospheric delay for microwaves from surface weather data. Radio Sci 22:379–386

Baby HB, Golé P, Lavergnat J (1988) A model for the tropospheric excess path length of radio waves from surface meteorological measurements. Radio Sci 23:1023–1038

Bevis M, Businger S, Herring TA, Rocken C, Anthes RA, Ware RH (1992) GPS-meteorological: remote sensing of atmospheric water vapor using the global positioning system. J Geophys Res-Atmos 97:15787–15801

Bevis M, Businger S, Herring TA, Rocken C, Anthes RA, Rocken C, Ware RH, Chiswell S (1994) GPS meteorology: mapping zenith wet delays onto precipitable water. J Appl Meteorol 33(3):379–386

Black HD (1978) An easily implemented algorithm for the tropospheric range correction. J Geophys Res 38(B4):1825–1828

Bock O, Doerflinger E (2001) Atmospheric processing methods for high accuracy positioning with the global positioning system. Phys Chem Earth (A) 26(6–8):373–383

Brunner FK, Welsch WM (1993) Effect of the troposphere on GPS measurements. GPS World 4(1):42–51

Chao CC (1972) A model for tropospheric calibration from daily surface and radiosonde balloon measurement. jet propulsion laboratory, Pasadena, California. Tech Memorandum 391–350:16

Cole AE, Court A, Kantor AJ (1965) Model atmospheres. In: Valley S (ed) Handbook of geophysics and space environments. McGraw-Hill, New York (also available from NTIS as ADA056800)

Davis JL, Herring TA, Shapiro II, Rogers AEE, Elgered G (1985) Geodesy by radio interferometry: effects of atmospheric modeling errors on estimates of baseline length. Radio Sci 20:1593–1607

Foelsche U, Kirchengast G (2001) A new "geometric" mapping function for the hydrostatic delay at GPS frequencies. Phys Chem Earth PT A 26(3):153–157

Goad CC, Goodman L (1974) A modified Hopfield tropospheric refraction correction model. AGU annual fall meeting, San Francisco, CA (Abstract: EOS 55: 1106)
Gregorius TLH, Blewitt G (1999) Modeling weather fronts to improve GPS heights: a new tool for GPS meteorology? J Geophys Res-Sol Earth 104(7):15261–15279
Griffith DJ (ed) (1999) Introduction to electrodynamics. Prentice Hall, Singapore
Herring TA (1992) Modeling atmospheric delays in the analysis of space geodetic data. In: Proceedings of the symposium on refraction of transatmospheric signal in geodesy, The Netherlands 36, New series: 157–164
Hofmann-Wellenhof B, Lichtenegger H, Collins J (eds) (2001) Atmospheric effect on the global positioning system, theory and practice. Springer, Berlin
Hopfield HS (1969) Two-quartic tropospheric refractivity profile for correcting satellite data. J Geophys Res 74(18):4487–4499
Ifadis IM (1992) The excess propagation path of radio waves: study of the influence of the atmospheric parameters on its elevation dependence. Surv Rev 31:289–298
Langley RB, Kleusberg A, Teunissen PJG (1996) Propagation of the GPS signals. In: GPS for geodesy. Lecture notes in earth sciences. Springer, Berlin, pp 103–140
Lanyi G (1984) Tropospheric delay effects in radio interferometry. Telecommunications and data acquisition progress. Jet Propulsion Laboratory, Pasadena, pp 152–159
Leick A (ed) (1995) GPS satellite surveying. Wiley, New York
Marini JW (1972) Correction of satellite tracking data for an arbitrary tropospheric profile. Radio Sci 7(2):223–231
Mendes VB, Langley RB (1998) Tropospheric zenith delay prediction accuracy for airborne GPS high-precision positioning. In: Proceeding of the institute of navigation, 54th annual meeting 1998, pp 337–347
Niell AE (1996) Global mapping functions for the atmosphere delay at radio wavelengths. J Geophys Res 101(B2):3197–3246
Niell AE (2000) Improved atmospheric mapping functions for VLBI and GPS. Earth Planets Space 52:699–702
Owens JC (1967) Optical refractive index of air: dependence on pressure, temperature and composition. Appl Opt 6:51–58
Saastamoinen J (1972) Introduction to practical computation of astronomical refraction. Bul Geodes 106:383–397
Seeber G (1993) Satellite geodesy, foundations, methods and applications. Walter de Gruyter, Berlin
Smith WL (1966) Notes on the relationship between total precipitable water and surface dew point. J Appl Meteorol 5:726–727
Smith EK, Weintraub S (1953) The constants in the equation of atmospheric refractive index at radio frequencies. Proc Inst Radio Eng 41(8):1035–1037
Suparta W (2008) Characterization and analysis of atmospheric water vapour using ground-based GPS receivers at Antarctica. Ph.D. thesis, Faculty of Engineering, Universiti Kebangsaan Malaysia
Suparta W, Abdul Rashid ZA, Mohd Ali MA, Yatim B, Fraser GJ (2008) Observations of Antarctic precipitable water vapor and its response to the solar activity based on GPS sensing. J Atmos Sol-Terr Phys 70:1419–1447
Thayer GD (1974) An improved equation for the radio refractive index of air. Radio Sci 9 (10):803–807
Wallace JM, Hobbs PV (1997) Atmospheric science an introductory survey. Academic Press, New York
World Meteorological Organization (2000) General meteorological standards and recommended practices. Appendix A, WMO technical regulations 49, corrigendum
Yuan L, Anthes R, Ware R, Rocken C, Bonner W, Bevis M, Businger S (1993) Sensing climate change using the global positioning system. Geophys Res 98(D8):14925–14937